ISSN(Online): 2320-9801
ISSN (Print): 2320-9798

International Journal of Innovative Research in Computer and Communication Engineering

(An ISO 3297: 2007 Certified Organization)

Website: www.ijircce.com

Vol. 5, Issue 5, May 2017

Saliency-based Feature Assessment for Color Deficients

Monali G. Meshram[1], A. M. Shah[2]

M. Tech. Student, Department of Electronics Engineering, Government College of Engineering, Amravati, India[1]

Assistant Professor, Department of Electronics Engineering, Government College of Engineering, Amravati, India[2]

ABSTRACT: The difference in pursuing colors happens because of photo pigments in retinal cones. It is hard to measure the one's ability to apprehend colored scenes and predict its effects on the behaviours. A method for measurement and apprehend information loss based on ability to predict visual scenes is developed here. This method is based on visual salience. A visual salience for color deficient is found out first, the corresponding loss of information is predicted from comparison of color deficient and normal observer.

KEYWORDS: Vision; Color deficiency; Saliency

I. INTRODUCTION

The extend of individual's experience somewhat depends on differences in perception of senses. Color-sensitive photo pigments change individual's perception of intricate visual scenarios. Therefore, individuals suffer through differences in visual perception. Most of the humans are trichromatic, i.e., colors are perceived by the population-activity of long-wavelength (L), middle-wavelength (M), and short-wavelength (S)-sensitive cones. Individuals lacking one set of photo pigments develop color discrimination; i.e., they are blind to the difference between a certain pair of colors, such as red or green. The genetic polymorphism is the major consequence of divergence in color vision. There are presently some practical methods to compensate such color-vision deficient (CD) observers medically so as to have common trichromatic vision; however gene therapies under development may shortly provide a cure. An alternative technique to potentiate visual accessibility for CD observers is the compensatory design of visual material with sufficient information to be perceived by all viewers, including CD observers.

In this study, visual saliency as an alternative to quantify perceptual differences is proposed. Visual salience concept was first proposed in the context of cognitive science, and later computational implementations were studied. Saliency is used to a great degree in studies on human visual attention; for example, many properties of bottom-up visual attention in trichromatic human observers are predicted by saliency models. Although the term "saliency" reflects different aspects of perceptual performance, which includes eye movements, in this study this term will be used to denote the visual conspicuity predicted from image parameters. Visual saliency potentially accounts for the complexity in the relationships between color vision and cognitive ability.

II. RELATED WORK

Approximately 200 million people worldwide are affected by color vision deficiency, where the individual's ability to effectively perform color and visualization-related tasks is compromised. In [6] author proposed a physiologically-based model for simulating color vision. This system is based on the stage theory of human color vision and the model is derived from data reported in electrophysiological studies. It is the first model to systematically handle normal color vision, anomalous trichromacy, and dichromacy in a unified way.

In a computerized simulation [3] of dichromatic vision, dichromat's color confusions and color palette are represented for normal trichromats. Because dichromatic vision deficiency of trichromatic vision, it should be possible to simulate the color gamut of dichromats for trichromatic observers. The simulation of dichromatic vision for the normal trichromat should not only reproduce the dichromat's color confusions but also provide a credible color appearance.

ISSN(Online): 2320-9801
ISSN (Print): 2320-9798

International Journal of Innovative Research in Computer and Communication Engineering

(An ISO 3297: 2007 Certified Organization)

Website: www.ijircce.com

Vol. 5, Issue 5, May 2017

Colorimetry helps in deducing the color confusions. Dichromacy is a type of color deficiency where one of any class of cones is absent and so dicromats can discriminate colors on the basis of the responses of the two remaining cone types. One of the three colorimetric components in terms of the L, M, and S-cone spectral responses is physiologically undetermined for a dichromat color vision. As the dichromat does not see any difference, this simulation result is chosen to imitate for the normal observer the appearance of colors for the dichromat. Color percepts of dichromats are used to this end. Based on these results, assumptions concerning the hues that appear to be same to dichromatic and to normal observers are presented. Color stimuli are defined on these common hues. First, it is assumed that neutrals for normals are perceived as neutrals for dichromats. Accordingly, no neutral stimuli are to be changed by the simulation. Second, unilateral inherited color vision deficiencies suggests that a stimulus of 575 nm is perceived as the same yellow, 475 nm as the same blue, by trichromats as by protanopes and deuteranopes. Third, for the case of unilateral acquired tritanopia, the corresponding two hues for a tritanope are a red with a dominant wavelength of 660 nm and a blue–green with a dominant wavelength of approximately 485 nm. From the results, the algorithm is defined where the replacement value of the physiologically ineffective LMS component is determined.

The proposed system is based on visual saliency, [10]-[17] suggets various saliency techniques, where saliency detection is based on k-means clustring [10], BMS computes saliency maps by analyzing the topological structure of Boolean maps which is based on Gestalt principle of figure-ground segregation [11], a regional contrast based saliency extraction algorithm which tests global contrast differences and spatial coherence [12], context-aware saliency detects the image regions that represent the scene [13], a pixel-accurate saliency map uniformly covers the objects of interest and separates fore- and background consistently [14], saliency map is used to detect real change regions between two remote sensing images of a given scene acquired at different times [15], super pixels on the saliency map where intensity of saliency map in each super pixel is used to compute distance between the centres of super pixels, this act as constraints to extract the objects from the image[16], saliency method exploits features of color and luminance [17].

III. PROPOSED SYSTEM

1. *MATHEMATICAL MODELING*

The saliency divergence is derived in the three steps. The first two steps can be applied to different visual processing models by changing their parameters.

a. Models of early sensory system

I. Opponent color maps

First, the early sensory encoding of color, luminance, and orientation, according to models of the cone distribution and subsequent opponent-color processing is predicted. The previously proposed simulation methods ([1] [3]) do not consider color opponency to simulate the color confusions experienced by dichromat observers. To link the cone configuration and later visual processing stage, the original model of visual salience [4] is extended by introducing a more biologically plausible model of color opponency in the early visual system (Table 1); here, the chromatic information is represented in the Derrington-Krauskopf-Lennie (DKL) color space, which reflects the preferences of retinal ganglion cells and lateral geniculate nucleus (LGN) neurons and may describe the bottom-up attention resulting from early visual processing.

Table 1
Models of early visual system for the individual color vision types

	Cones			**Opponent signals**		
	S	M	L	"blue-yellow"	"red-green"	luminance
Protanope	*	*	-	S-M	-	M
Deuteranope	*	-	*	S-L	-	L
Tritanope	-	*	*	-	L-M	L+M
Common	*	*	*	S-(L+M)	L-M	L+M

ISSN(Online): 2320-9801
ISSN (Print): 2320-9798

International Journal of Innovative Research in Computer and Communication Engineering

(An ISO 3297: 2007 Certified Organization)

Website: www.ijircce.com

Vol. 5, Issue 5, May 2017

II. Orientation maps

The orientation maps were derived from the output of the luminance signal. The orientation filters were products of von Mises orientation selectivity and log- Gaussian spatial frequency selectivity, which well describe the neural receptive fields in the early visual cortex:

$$\omega_{ij}(k) = e^{k\cos(\angle k-\theta_i)} e^{-\frac{1}{2}\left(\frac{\ln(||k||-\phi_j)}{\sigma}\right)^2} \quad (1)$$

Where ω_{ij} is the filter weight that peaked at the ith orientation and jth spatial frequency(θ_i, ϕ_j). k denotes a wave vector in the spatial frequency space that was derived with a 2D Fourier-transform, k and $|k|$ respectively represent its orientation and absolute value. The tuning parameters were set as k = 3 and σ = .5, which roughly approximated the tuning property in the primary visual cortex. Multiplying the above weight function in the spatial frequency space simulates convolution of image with a receptive field that is sensitive to local orientation within images. The four orientation bands (vertical, horizontal, and two diagonal orientations) and four spatial scales is used. The effect of varying the number of spatial scales in the additional analysis is also explored. Variation in other major parameters (increasing the number of the orientation bands, or eliminating the highest or the lowest spatial scale) did not yield any qualitative changes. Temporal features is not extracted since only static images are used.

b. Derivation of Saliency Maps:

I. Center-surround antagonism

Saliency maps were constructed based on the aforementioned models of early sensory responses. The maps of different modalities (color, luminance, and orientation) were first independently processed by multiscale center-surround antagonistic filters. First, the local features in the luminance, chromatic, and orientation maps were extracted with center-surround antagonism (CSA) filters. After pixel-wise square rectification of each modality map, CSA filters were applied on multiple spatial scales by decomposing the image. Again we used log-Gaussian-type band-pass filters, which can capture the scale-free property of natural images. The CSA filter was defined in the spatial frequency space as follows:

$$CSA_l(k) = \exp\left(-\frac{1}{2}\left(\frac{\ln(||k|| - \psi_l)}{s}\right)^2\right) \quad (2)$$

Where ψ_l is the spatial frequency at which the lth filter has its peak weight. The peak spatial frequency of the finest band-pass filter, $\psi_l$was matched to a visual angle of 15 cycles/deg (approximately equal to the half limit resolution of an observer with a visual acuity of 1.0). The lower spatial frequency bands had peak weights at the halves of the nearest higher frequency bands, i.e., $\psi_l = \frac{\psi_{l-1}}{2}(l = 2,3,4,\dots.)$. The smallest spatial-pooling scale (the peak frequency of the finest band-pass filter) corresponds to pooling within a disc of diameter 0.07^o. Multiplying these functions in the frequency space simulates the convolution of Mexican- hat filters across a feature map, which extracts local contrasts of the spatial configuration of the feature of the feature on multiple scales.

II. Saliency map

Next, individual CSA filter outputs are inverse-Fourier transformed and square-rectified, in order to produce feature maps $f_l(r)$ of pixel location r for different spatial scales l. Individual pixels within-scale feature maps were summed up across all spatial scales (L-M and S components are summed up to derive a color feature map), before they were normalized (*i.e.*, divided by the sum of the values within whole image):

$$f(r;m) = \frac{\sum_l f_l(r;m)}{(\sum_r \sum_l f_l(r;m))^c} \quad (3)$$

Where the parameter c controlled the effectiveness of the normalization; $c = 1$ is set for the main analysis. This normalization procedure mimics the neuronal gain control in the visual pathway. The results are feature maps for color modality (color, luminance and orientation). Finally, the luminance, color feature maps are unified into single saliency map by computing their weighted sum for each pixel: $S(r) = \sum_m F(r;m)$. Weights of the summation are set to 1 of the

ISSN(Online): 2320-9801
ISSN (Print): 2320-9798

International Journal of Innovative Research in Computer and Communication Engineering

(An ISO 3297: 2007 Certified Organization)

Website: www.ijircce.com

Vol. 5, Issue 5, May 2017

luminance and chromatic maps. This unified saliency map was again normalized by the sum of values within the whole image, and this yielded the final saliency map at pixel r in image I for an observer O_i: $P(r|O_i;I) = S(r)/\sum_r S(r)$, as a probability distribution.

III. Quantification of saliency loss

Finally, a spatial distribution of saliency loss is obtained by comparing the two different saliency maps between groups (normal vs. CD). We quantified the local information loss (or gain) value L for observer O_i compared with another arbitrary observer O_j as

$$L(r;I) = P(r|O_i;I) - P\left(r\middle|O_j;I\right) \quad (4)$$

Here the loss of information is calculated between dichromat and trichromat observer.

2. EXPERIMENTAL MODELING

I. Software module

The following flow diagram is for the system implemented on the MATLAB

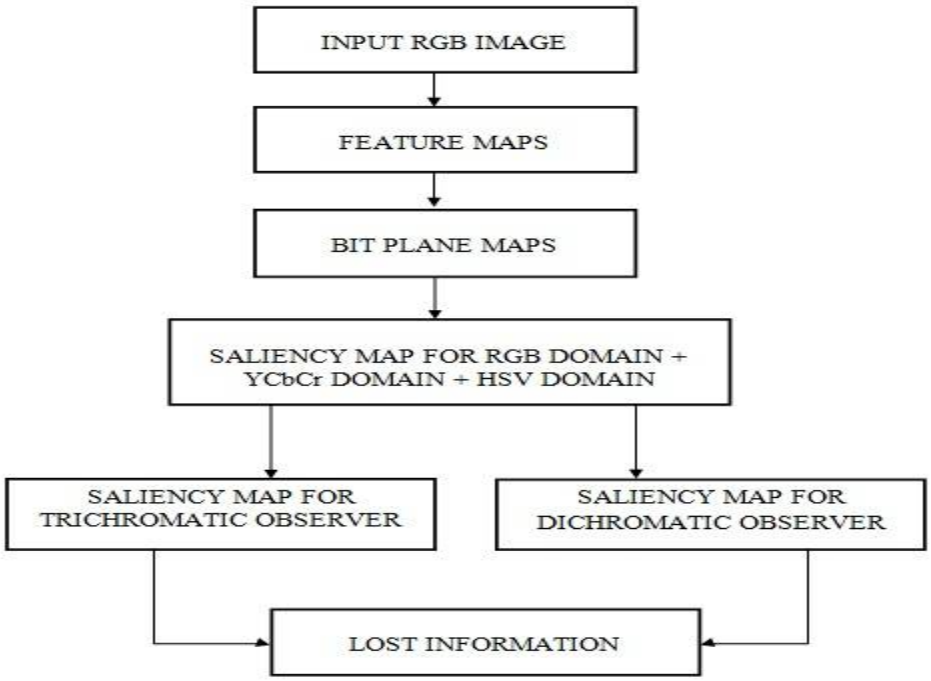

Figure 1: Flow diagram for the system implemented on MATLAB

1. *Image:* In the MATLAB workspace, most images are represented as two-dimensional arrays (matrices), in which each element of the matrix corresponds to a single pixel in the displayed image. For example, an image composed of 200 rows and 300 columns of different colored dots stored as a 200-by-300 matrix. Some images, such as RGB, require a three-dimensional array, where the first plane in the third dimension represents the red pixel intensities, the second plane represents the green pixel intensities, and the third plane represents the blue pixel intensities.

ISSN(Online): 2320-9801
ISSN (Print): 2320-9798

International Journal of Innovative Research in Computer and Communication Engineering

(An ISO 3297: 2007 Certified Organization)

Website: www.ijircce.com

Vol. 5, Issue 5, May 2017

2. *Feature maps*: A feature maps are been calculated for obtaining different maps for color opponent maps and luminance map. An Image given as input in first block act as output for this block, considering different features maps are calculated.
3. *Bit plane maps:* Bit plane maps are calculated from different feature map contents as R, G, B, RG, BY, where these components of image are considered as inputs. Depending upon size of image bit plane maps are calculated. Generally, for 8 bit image, 8 bit planes are computed.
4. *Rough saliency map* : Considering the edge is getting clearer in every bit plane map, the clearer edge in the last bit plane map is considered as input, wherein mean of entire image is considered, applying conditions of mean of an image, rough saliency map is derived.
5. *Saliency map RGB*: The saliency map is calculated in RGB color domain.
6. *Saliency map YCbCr*: As the saliency map for RGB domain is calculated, similarly it is calculated for YCbCr domain, where luminance and chrominance component of an image is considered.
7. *Saliency map HSV*: As the saliency map for RGB domain is calculated, similarly it is calculated for HSV domain, where hue and saturation value of an image is considered.
8. *Super saliency map*: Combining the saliency maps of RGB, YCbCr and HSV domain, super saliency map is calculated. The super saliency map is calculated for trichromatic observer. Using the same algorithm saliency map for dichromatic observer is calculated.
9. *Information loss:* The saliency map is derived for trichromatic observer first; similarly it is calculated for dichromatic observer. The difference between the two maps gives the information loss *i.e.* loss of color information by color deficient.

II. Hardware module

The similar system can be implented on Altera DE2 board, the flow diagram for the same can be seen below;

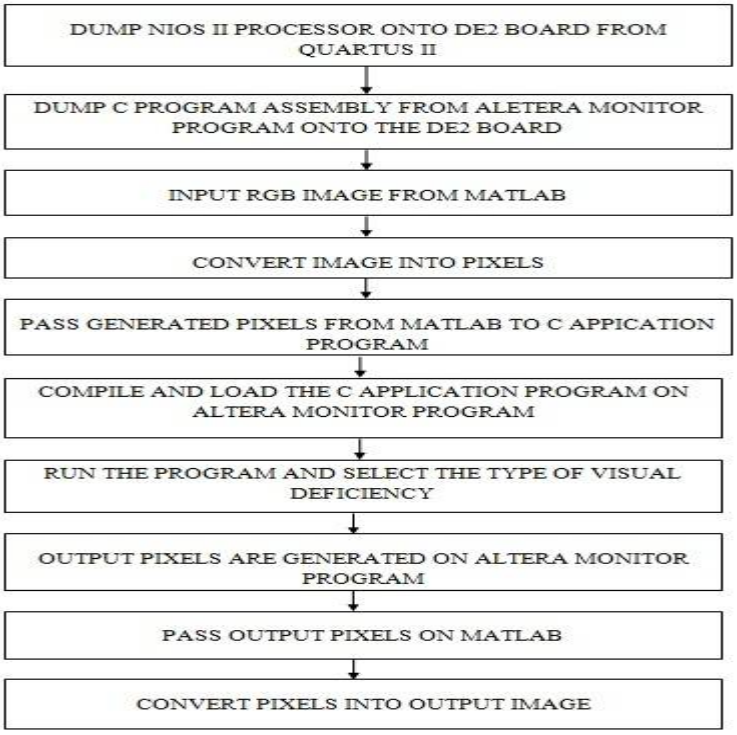

Figure 2: Flow diagram for the system implemented on Altera DE2 board

ISSN(Online): 2320-9801
ISSN (Print): 2320-9798

International Journal of Innovative Research in Computer and Communication Engineering

(An ISO 3297: 2007 Certified Organization)

Website: www.ijircce.com

Vol. 5, Issue 5, May 2017

In order to process image on Altera DE2 NIOS II, image is taken from MATLAB platform. With thousands of pixels to keep track of, it can be downright scary to the occasional programmer. The image is broke down to pixels. To start with, if use a RGB picture of size 480×640 of 32 bit, each of the pixels in a picture has one value. Instead of pixels we get 2D array, this 2D array is stored in a text file. Now that images are basically 2D arrays, we have to create image object in C application program in NIOS II processor. The output image pixels created from NIOS II processor over C compiler needs to get back on MATLAB platform to form the processed output image.
Contents for the system development are as follows;

- Nios II System
- Altera's SOPC Builder
- Integration of the Nios II System into a Quartus II Project
- Running the Application Program

IV. SIMULATION RESULTS

1. RESULT ON SOFTWARE MODULE

The model not only differentiates the saliency map for tritanopes from the other two dichromatic visions, but also yields slightly different predictions. This is because the difference in cone combination (i.e., L and S, or M and S) can lead to different luminance signals, in addition to the primary effect of lacking an L-M signal. This fact indicates that the current approach is potentially able to differentiate perceptions resulting from different types of color deficiency. The saliency map is derived for trichromatic observer first; similarly it is calculated for dichromatic observer. The difference between the two maps gives the information loss.

Figure 3 : Result of Information loss on software module for Protanopia, Deuteranopia and Tritanopia respectively.

2. RESULTS ON HARDWARE MODULE

Considering the experimental modelling of the proposed system for hardware modelling, if we consider image of size 480×640 of size 64 bit and 32 bit, the output image we get is as follows,

ISSN(Online): 2320-9801
ISSN (Print): 2320-9798

International Journal of Innovative Research in Computer and Communication Engineering

(An ISO 3297: 2007 Certified Organization)

Website: www.ijircce.com

Vol. 5, Issue 5, May 2017

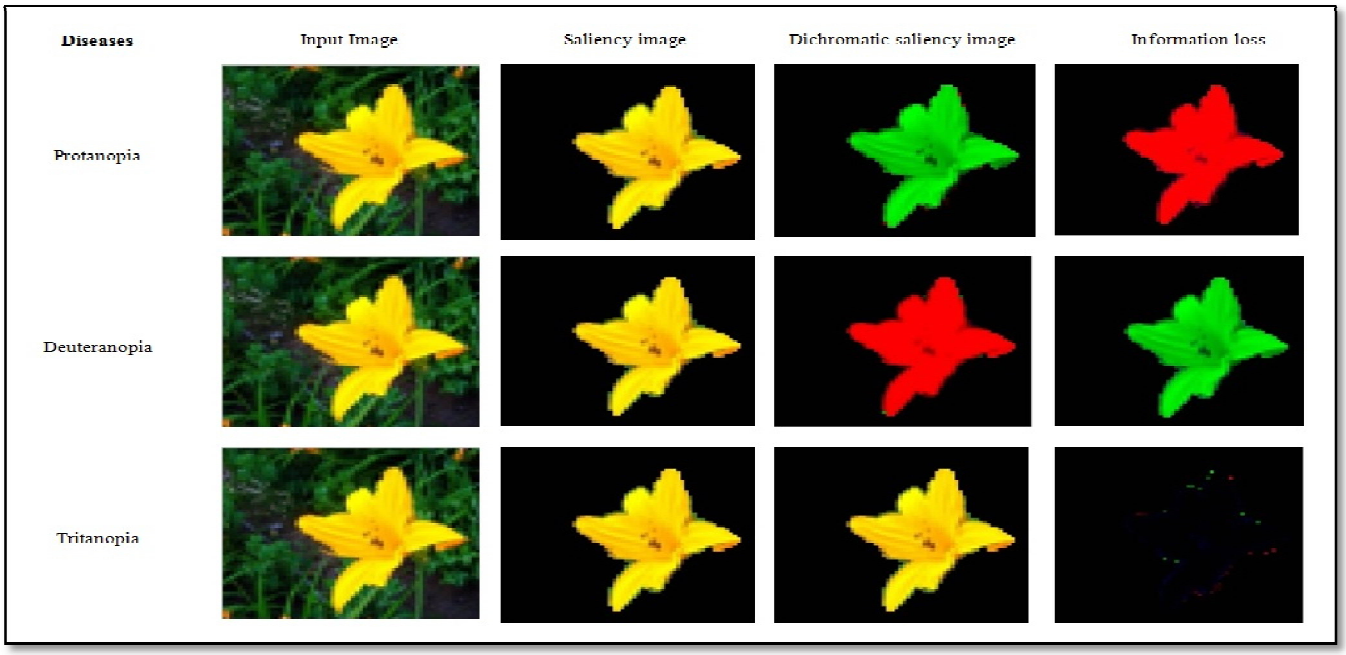

Figure 4: Result of Information loss on hardware module for Protanopia, Deuteranopia and Tritanopia respectively for 64 bit image.

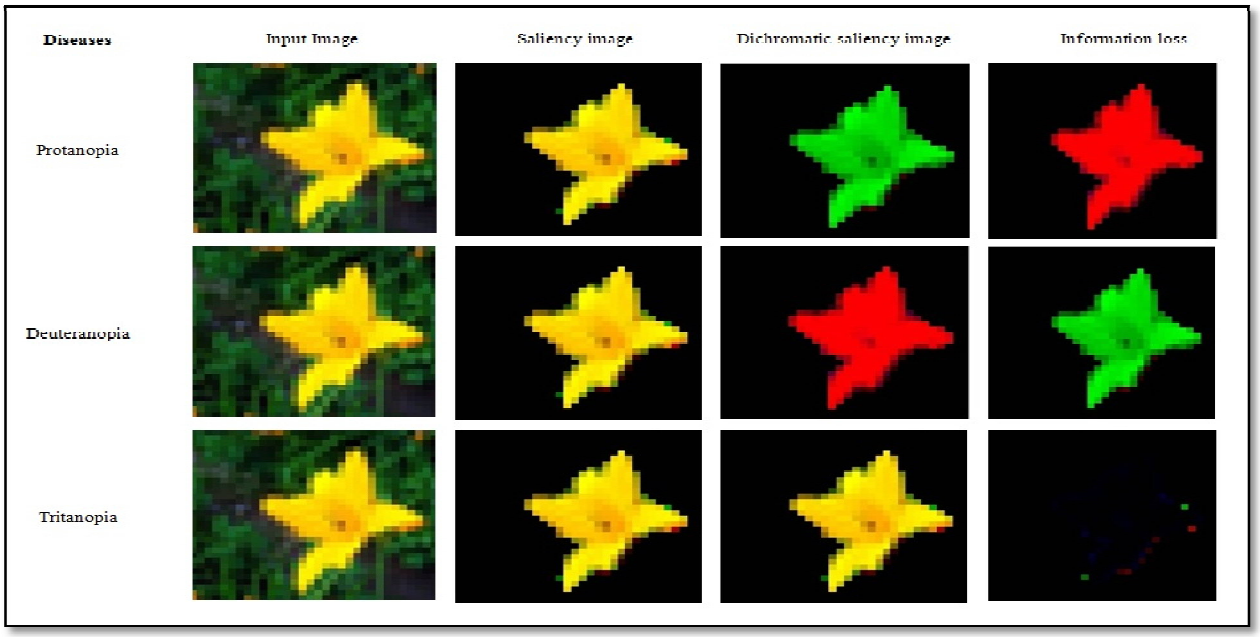

Figure 5: Result of Information loss on hardware module for Protanopia, Deuteranopia and Tritanopia respectively for 32 bit image.

ISSN(Online): 2320-9801
ISSN (Print): 2320-9798

International Journal of Innovative Research in Computer and Communication Engineering

(An ISO 3297: 2007 Certified Organization)

Website: www.ijircce.com

Vol. 5, Issue 5, May 2017

V. PERFORMANCE ANALYSIS

1. *Precision calculation*

In software and hardware modules, the comparison of the average saliency judgments of the control and CD observers was consistent with predictions of the model. These results support the plausibility of the deuteranope simulation and the saliency loss model for revealing individual differences in color perception.
Precision is calculated to see how the object of interest is been cropped from the image. The precision is applied over software and hardware modules.
Considering different set of images applied for software and hardware module, we could actually form a judgement between the two methods. However, the time for simulation for hardware module is considerably more, because of having every pixel of the image being processed. If the average precision is calculated considering different set of images it comes out nearly 90 % for both the modules.

2. *Execution time analysis*

For processing of 32 bit image, hardware based algorithm the number of pixels to be processed on Altera DE2 board is 32×32×3 = 3072 while for 64 bit image, it is 64×64×3 = 12280, so the processing time for 64 bit image is more compared to that of 32 bit image, even the resolution of image can be increased or decreased. If width and height of image is changed then processing time is also varied accordingly. This processing time is also depends on system processor. If advanced processor is used for the given application, then time required for the execution will be very less. So, generally high end processing system is preferred over low processing system.

V. CONCLUSION

To date, there is no established color space model for dichromats or anomalous trichromats, although some studies suggest that “red” and “green” can be discriminated through variations in the optical density of pigments. In this study, we simply assumed that the color opponency of the missing cone type is absent. This is a parsimonious model that follows basic findings in the anatomical connectivity in the early visual systems and a previously verified model. The point of this model is to introduce the information loss at the level of opponent color coding. The current model can nevertheless provide a practical approximation of saliency loss for a broad class of so-called “red-green” color vision deficiency.
The model is implemented on complete software platform on MATLAB and hardware platform on Altera DE2 board (NIOS II processor). Based on the performance analysis it is found that the precision for hardware module is more than software module and if the resolution of an input image is increased; the time for the processing is increased.

REFERENCES

1. F. Viénot, H. Brettel, L. Ott, A. Ben M’Barek, and J. D. Mollon, “What do color-blind people see?” , Nature , vol. 376, no. 6536, pp. 127–128, 1995.
2. J. Neitz, M. Neitz, and P. M. Kainz, “Visual pigment gene structure and the severity of color vision defects”, Science , vol. 274, no. 5288, pp. 801–804, Nov. 1996
3. H. Brettel, F. Vienot and J. D. Mollon, “Computerized simulation of color appearance for dichromats”, Journal of the Optical Society of America A, Optical , vol. 14, no. 10, pp. 2647-2655, Oct. 1997.
4. L. Itti and C. Koch, “Computational modeling of visual attention,” Nature Reviews Neuroscience, vol. 2, no. 3, pp.194–203, 2001. , 2009.
5. K. Mancuso et al., “Gene therapy for red–green colour blindness in adult primates,” Nature, vol. 461, pp. 784–787, Oct. 2009.
6. G. M. Machado, M. M. Oliveira and L .A. F. Fernandes, “A physiologically-based model for simulation of color vision deficiency”,IEEE Transaction Visual Computation Graphics , vol. 15, no. 6, pp. 1291-1298, Nov./ Dec. 2009.
7. J. Neitz and M. Neitz, “The genetics of normal and defective color vision,” Vision Research, vol. 51, no. 7, pp. 633–651, Apr. 2011.
8. Satohiro Tajima, Kazutera Komine, “Saliency-Based Color accessibility”, IEEE Transactions on Image Processing, Vol.24, No.3, pp.1115 – 1126, 2015.
9. Jyoti Verma, Vineet Richhariya, “A Survey Paper On An Efficient Salient Feature Extraction By Using Saliency Map Detection With Modified K-Means Clustering Technique”, International Journal Of Communication And Computer Technologies, Volume 01-No.5, Issue: 02, 2012.

ISSN(Online): 2320-9801
ISSN (Print): 2320-9798

International Journal of Innovative Research in Computer and Communication Engineering

(An ISO 3297: 2007 Certified Organization)

Website: www.ijircce.com

Vol. 5, Issue 5, May 2017

10. Jianming Zhang, Stan Sclaroff, "Exploiting Surroundedness for Saliency Detection: A Boolean Map Approach" IEEE Transactions on Pattern Analysis and Machine Intelligence, Volume: 38, No. 5, pp. 889 - 902, 2016.
11. Ming-Ming Cheng, Niloy J. Mitra, Xiaolei Huang, Philip H. S. Torr, Shi-Min Hu, "Global Contrast Based Salient Region Detection", IEEE Transactions on Pattern Analysis and Machine Intelligence, Volume: 37, Issue: 3, pp. 569 – 582, 2015.
12. Stas Goferman, Lihi Zelnik-Manor, Ayellet Tal, "Context-Aware Saliency Detection", IEEE Transactions on Pattern Analysis and Machine Intelligence, Volume: 34, Issue: 10, pp. 1915 – 1926, 2012.
13. Federico Perazzi, Philipp Krahenbuhl, Yael Pritch, Alexander Hornung, "Saliency Filters: Contrast Based Filtering for Salient Region Detection", IEEE Conference on Computer Vision and Pattern Recognition (CVPR), 978-1-4673-1226-4, 2012.
14. Minghui Tian, Shouhong Wan, Lihua Yue, "A Novel Approach for Change Detection in Remote Sensing Image Based on Saliency Map", Computer Graphics, Imaging and Visualisation, 0-7695-2928-3, 2007.
15. Srikanth Muralidharan, Arun Balajee Vasudevan, Chintapalli Shiva Pratheek, Shanmuganathan Raman, "A novel approach to the extraction of multiple salient objects in an image", IEEE International Conference on Signal Processing Informatics, Communication and Energy Systems (SPICES), 978-1-4799-1824-9, 2015.
16. Radhakrishna Achantay, Sheila Hemamiz, Francisco Estraday, and Sabine Susstrunky, "Frequency-tuned Salient Region Detection", IEEE Conference on Computer Vision and Pattern Recognition, 978-1-4673-4527-9, 2009.
17. A website: Altera Development and Education Board Manual: Altera kit Information Source, May 21, 2017. A www.usna.edu/EE/ec463/docs/DE2-70-Manual.pd

BIOGRAPHY

Monali G. Meshram is Master of Technology (Electronic and Systems Communication) student in the Electronics Engineering Department, Government College of Engineering, Amravati. She received Bachelor of Technology (Electronics and Telecommunication) degree in 2014 from Government College of Engineering, Amravati, MS, India. Her research interests are Image processing, VLSI etc.

A. M. Shah is Assistant Professor in the Electronics Engineering Department, Government College of Engineering, Amravati. He received Bachelor of Technology (Electronics and Telecommunication) degree in 2004 from SGB University, Amravati and Master of Technology (VLSI) in 2008 from RTM University, Nagpur.